Journal of Natural Pesticide Research 16 (2026) 100191

Contents lists available at ScienceDirect

Journal of Natural Pesticide Research

journal homepage: www.journals.elsevier.com/journal-of-natural-pesticide-research

Spatiotemporal profiling of bioactive metabolites in a resilient plant species and its antifungal potential against plant pathogens

M. Gabriela Mattera [a,b,1,*], Estefanía Butassi [c,2], Federico Ferreres [d,3], Melina Di Liberto [c,4], Mónica Hourcade [e,5], Laura Svetaz [c,6,7], Araceli Bader [b,8], Diego A. Moreno [f,9]

[a] Forestry and Agricultural Research Institute of Bariloche, IFAB (INTA Bariloche-CONICET), S.C. Bariloche, Argentina
[b] Present address: Instituto de Investigaciones en Biodiversidad y Biotecnología (INBIOTEC-CONICET) y Fundación para Investigaciones Biológicas Aplicadas (FIBA), Mar del Plata, Argentina
[c] Laboratorio de Bioprospección de Productos Antimicrobianos, Facultad de Ciencias Bioquímicas y Farmacéuticas, Universidad Nacional de Rosario, Santa Fe, Argentina
[d] Department of Food Technology and Nutrition, Molecular Recognition and Encapsulation (REM) Group, Universidad Católica de Murcia. UCAM, Campus Los Jerónimos, s/n., Murcia 30107, Spain
[e] Laboratorio CGEM, Facultad de Ciencias Bioquímicas y Farmacéuticas, Universidad Nacional de Rosario, Santa Fe, Argentina
[f] Laboratorio de Fitoquímica y Alimentos Saludables (LabFAS), CSIC, CEBAS, Campus Universitario de Espinardo-25, Murcia 30100, Spain

ARTICLE INFO

Keywords:
Azorella prolifera
Secondary metabolites
Antifungal activity
Crop protection
Plant-based approach

ABSTRACT

Concerns about the ecological and health risks of indiscriminate use of pesticides have increased interest in natural alternatives that are less harmful yet still effective. Resilient species from harsh environments are a valuable source of active compounds. However, intraspecific chemical variability resulting from the interaction between local growing condition and plant developmental stage is often underestimated, despite its relevance for identifying superior raw materials. *Azorella prolifera,* a widely dominant species in arid and semiarid areas of South America, is a valuable model for addressing this purpose. This study aimed to carry out a spatiotemporal characterization of bioactive metabolite profiling of *A. prolifera*, considering different provenances and phenological stages of the plant material. The antifungal activity of *A. prolifera* essential oils and hydrolats against nine plant fungal pathogens was also assessed. This species exhibited a rich secondary metabolite profile, containing at least 31 (poly)phenols (4.1 ± 1.4 g/100 g of dry weight) and up to 55 volatiles. *A. prolifera* essential oils showed a promising performance against *Fusarium graminearum* (a devastating crop pathogen), with minimum inhibitor and fungicide concentrations between 250 and 500 µg/mL. Variability in both chemical profiling and antifungal effectiveness within this species was revealed. Natural populations from 41°08'S - 71°08'W provide an additional value, as their hydrolats exhibited fungistatic activity against *A. fumigatus* and *B. cinerea* fungi. Our results highlight the potential of *A. prolifera* for biofungicide formulation and demonstrate the importance of spatiotemporal chemical screening of raw materials to identify superior ones.

* Correspondence to: Instituto de Investigaciones en Biodiversidad y Biotecnología (INBIOTEC-CONICET) y Fundación para Investigaciones Biológicas Aplicadas (FIBA), Vieytes 3103, Mar del Plata CP 7600, Argentina.
E-mail address: mattera.mg@gmail.com (M.G. Mattera).
[1] 0000-0002-7062-050X
[2] 0009-0008-7248-5357
[3] 0000-0002-8682-0004
[4] 0000-0003-4630-6032
[5] 0009-0002-1712-9751
[6] *Author deceased*
[7] 0000-0002-1023-1641
[8] 0000-0002-3787-5914
[9] 0000-0002-6547-8764

https://doi.org/10.1016/j.napere.2026.100191
Received 20 January 2026; Received in revised form 1 April 2026; Accepted 17 April 2026
Available online 20 April 2026

1. Introduction

The prolonged and indiscriminate use of chemical-based pesticides in agriculture has led to detrimental effects on ecosystems and human health worldwide (Tang et al., 2025). Moreover, the emergence of weed and pest resistance to agrochemicals is becoming increasingly widespread (Tang et al., 2025). Therefore, a global shift towards eco-friendly approaches combined with integrated management strategies for crop protection is urgently needed. In this context, plant-derived biocontrol approaches represent a promising pathway toward sustainable agricultural practices (Aremu et al., 2024).

Harsh environments with limiting growing conditions often exhibit poor vegetation cover but not necessarily reduced biodiversity (Carrasco-Puga et al., 2021) and may constitute valuable sources of bioactive compounds. Resilient species growing in these ecosystems have developed metabolic and physiological adaptations that enable them to withstand extreme conditions (Eshel et al., 2021), synthesizing a wide range of secondary metabolites to cope with abiotic and biotic stresses (You and Chan, 2015; Adhikary and Dasgupta, 2023). Moreover, plant chemical profiles may vary according to phenological stage and plant-environment interaction (Petrén et al., 2024). This variability can directly influence the biocontrol efficacy of plant-derived extracts.

Azorella prolifera (Cav.) G.M. Plunkett & A.N. Nicolas (synonym: *Mulinum spinosum* (Cav.) Pers.), commonly known as 'neneo', represents a clear example of an extremely resilient plant species, as it is dominant in the arid and semiarid environments of the Extra- Andean Patagonia areas (Ferreyra and Ezcurra, 2022). This species grows in a broad range of environments, including flat steppes, mountain slopes and summits, from near sea-level to 4000 m a.s.l (Fernández et al., 2017). It has adapted to withstand extreme cold, drought, desiccation, and high UV exposure. Traditionally, *A. prolifera* has been used by native Patagonian inhabitants to treat urinary disorders, dental neuralgias, liver diseases and altitude sickness (Molares and Ladio, 2014). In addition, anti-parasitic, analgesic, and anti-inflammatory properties have been reported for this species (Molares and Ladio, 2014; Estomba et al., 2006; Sülsen et al., 2006). Chemical studies of the aerial parts of this species have identified resin acids, α- and β-pinene, and limonene, as well as mulinane-type diterpenoids (Nicoletti et al., 1996). Both organic and aqueous extracts have shown *in vitro* trypanocidal activity against *Trypanosoma cruzi*, the causative agent of "Chagas" disease (Sülsen et al.,

Table 1
*R*t, UV and MS: $[M-H]^-$ and $MS^2[M-H]^-$ data of compounds from seeds and aerial part at different phenological stage of *A. prolifera.*[1].

	Compounds[2]	Rt (min)	UV (nm)	[M-H]⁻ *m/z*	MS^2 *mz*(%)	Sample
			Cinnamoyl acids			
2	5-CQA	15.7	298sh, 324	353	191(100), 179(5)	C_Veg, N_Flb, E_Flb, N_Flw, E_Flw, N_seeds, E_seeds
3	4-CQA	16.1	298sh, 324	353	173(100)	C_Veg, N_Flb, E_Flb, N_Flw, E_Flw, N_seeds, E_seeds
4	Caff-hexoside	17,7	———	341	179(90), 137(100)	C_Veg, E_Flb, E_Flw
5	5-CQA isom	18.8	———	353	191(100), 179(3)	C_Veg, E_Flb, E_Flw, N_seeds, E_seeds
6	CQA der	19.5	298sh, 330	797	635(100)[3]	C_Veg, E_Flb, N_Flw, E_Flw
8	5-FQA	22.0	298sh, 324	367	191(100)	C_Veg, E_Flb, E_Flw
11	4-FQA	23.2	298sh, 326	367	173(100)	C_Veg, N_Flb, E_Flb, N_Flw, E_Flw
24	3,5-diCQA	28.8	294sh, 326	515	353(100)	C_Veg, N_Flb, E_Flb, N_Flw, E_Flw, N_seeds, E_seeds
27	3,4-diCQA	30.1	294sh, 326	515	353(100)	C_Veg, N_Flb, E_Flb, N_Flw, E_Flw, N_seeds, E_seeds
30	Malonyl-diCQA	31.8	294sh, 327	601	557(40), 515(100)[4]	N_Flb, E_Flb, N_Flw, E_Flw
			Flavonoid-*O*-diglycosides			
10	Qct-3-*O*-gentiobioside	22.9	255, 266sh, 298sh, 354	625	301(100)	C_Veg, E_Flb, N_Flw, E_Flw, N_seeds, E_seeds
13	Qct-3-*O*-(6-pentosyl) hexoside	24.9	256, 268sh, 300sh, 354	595	301(100)	N_Flb
14	Kpf-3-*O*-gentiobioside	25.2	266, 345	609	285(100)	E_Flb, N_Flw, E_Flw, E_seeds
15	Qct-3-*O*-rutinoside (rutin)	25.3	———	609	301(100)	C_Veg, N_Flb, E_Flb, N_seeds, E_seeds
18	Isorh-3-*O*-gentiobioside	25.8	256, 266sh, 300sh, 354	639	315(100)	C_Veg, E_Flb, N_Flw, E_Flw, N_seeds, E_seeds
23	Isorh-3-*O*-rutinoside	28.0	255, 266sh, 352	623	315(100)	C_Veg, N_Flb
			Flavonoid-*O*-monoglycosides			
12	Eridct-hexoside	24.7	290, 330sh	449	287(100)	C_Veg, E_Flb, N_Flw, E_Flw, N_seeds
16	Eridct-hexoside isom	25.4	———	449	287(100)	C_Veg, E_Flb, E_Flw, N_seeds
19	Qct-3-*O*-hexoside	26.4	256, 266sh, 300sh, 352	463	301(100)	C_Veg, E_Flb, N_Flw, E_Flw, N_seeds, E_seeds
25	Isorh-3-*O*-hexoside	29.1	255, 266sh, 352	477	314(100)	C_Veg, E_Flb, N_Flw, E_Flw, N_seeds, E_seeds
22	Qct-3-*O*-(acetyl) hexoside	27.9	——	505	463(15), 301(100)	N_seeds, E_seeds
29	Isorh-3-*O*-(acetyl) hexoside	31.2	255, 266sh, 300sh, 354	519	315(100)	C_Veg, E_Flb, N_Flw, E_Flw, N_seeds, E_seeds
			Flavonoid-*C*-glycosides			
9	TtOHFlv-6-C-hexoside	22.4	256sh,267, 298sh, 350	447	429(30), 357(87), 327(100)	C_Veg, E_Flb, N_Flw, E_Flw, N_seeds, E_seeds
17	Apig-8-*C*-hexoside	25.4	270, 336	431	413(5), 341(30), 311(100)	C_Veg, E_Flb, N_Flw, E_Flw, N_seeds, E_seeds
20	TtOHFlv-*C*-(acetyl) hexoside	26.7	———	489	429(20), 357(30), 327(100)	C_Veg, E_Flb, N_Flw, E_Flw, N_seeds, E_seeds
26	Apig-*C*-(acetyl) hexoside	29.5	270, 334	473	413(10), 341(30), 311(100)	C_Veg, E_Flb, N_Flw, N_seeds, E_seeds
			Others Flavonoids			
7	Sinp-Isorh(acetyl) hexoside	21.5	254,266sh, 300sh, 345	725	681(45), 519(100)[5]	C_Veg, E_Flb, N_Flw, E_Flw
21	Qct-3-*O*-hexosyl derv	27.8	256, 266sh, 300sh, 354	607	545(10), 505(50), 463(100)[6]	N_Flb
28	Isorh-3-*O*-hexosyl derv	30.8	255, 266sh, 298sh, 350	621	559(40), 519(60), 477(100), 315 (35)	N_Flb

[1] Main observed fragments. Other ions were found but they were not included. [2]CQA: caffeoylquinic acid; FQA: feruloylquinic acid; Qct: quercetin; Apig: apigenin; Kpf: kaempferol; Caff: caffeoyl, Isorh: isorhamnetin; Eridct: eriodictyol; TtOHFlv: tetrahydroxyflavone; Sinp: sinapic acid. [3]MS^3(797→635): 461(85), 353(95), 191(100). [4]MS^3(601→515): 353(100). [5]MS3(725→519): 314(100). [6]MS^3(607→463): 301(100). C_Veg: sample from 41°08'S - 71°08'W at the vegetative stage; N_Flb: sample from 39°53'S - 70°42'W at the floral button stage; E_Flb: sample from 41°05'S - 70°49'W at the floral button stage; N_Flw: sample from 39°53'S - 70°42'W at flowering stage; E_Flw: sample from 41°05'S - 70°49'W at flowering stage; N_seeds: seeds from 39°53'S - 70°42'W; E_seeds: seeds from 41°05'S - 70°49'W.

2006). Antibacterial activity of organic extracts has also been reported (Nicoletti et al., 1996). Despite the ecological relevance of *A. prolifera* and its potential as a source of bioactive compounds, information on its metabolic profiling remains limited. Moreover, the potential association between chemical variability and fungicidal activity of its extracts has not yet been explored. Therefore, the present study aimed to characterize the secondary metabolite profiles of *A. prolifera* at different phenological stages across distinct natural populations. Additionally, the antifungal activities of the essential oils and their corresponding hydrolats, obtained from different provenances and phenological stages, were comparatively evaluated against phytopathogenic fungi.

2. Materials and Methods

2.1. Plant material

Aerial parts and seeds of 10 individuals of *A. prolifera* were randomly collected during two consecutively growing seasons (October 2021–February 2022 and October 2022- February 2023) from different sites. Three natural populations (IDs: N, C, E) were sampled in a 350 km North-South transect between 39°53'S to 41°7'S (Table 1). An extra population located at 40°53'S-68°03'W (E2) was included in Section 2.5. The sites were chosen considering latitudinal and longitudinal gradients that reflect diverse environmental conditions. In addition, three phenological stages of the *A. prolifera* aerial parts were considered in the analysis: vegetative (Veg), flower bud (Flb), and flowering (Flw). A minimum distance of 30 m between sampled individuals was maintained to avoid sampling closely related plants. The harvested material was then freeze-dried, ground and stored at – 20 ºC until preparation of the organic extract.

2.2. (Poly)phenolic extraction procedure

Organic extraction was carried out following the methodology described by Gironés-Vilaplana *et al.* (Gironés-Vilaplana et al., 2012). with some modifications. A mix of methanol, formic acid, and water (25:1:24) was used as extraction solvent (ES). One and a half milliliters of ES were added to 100 mg of ground material, homogenized by vortex, sonicated for one hour and kept at 4 °C overnight. Then, samples were centrifuged at 10,000 rpm (model Sigma 1–13, B. Braun Biotech International, Osterode, Germany) for 15 min and the supernatant was collected and transferred to a new microtube. The extraction process was repeated three times. All organic extracts from each sample were then pooled, filtered through a 0.45 μm PVDF filter (Millex HV13, Millipore, Bedford, Mass., USA) and transferred to the HPLC-vials. Three replicates of each sample were included in the analysis.

2.3. Identification of phenolic compounds

The bioactive compounds present in the organic extract of *A. prolifera* were identified by HPLC–DAD–ESI/MS^n analysis. An Agilent HPLC 1100 series model equipped with a photodiode array and a mass detector in series (Agilent Technologies, Waldbronn, Germany) was used. The HPLC system was controlled by ChemStation software (Agilent, version 08.03). The mass detector was an ion trap spectrometer (model G2445A) equipped with an electrospray ionization interface. The ionization conditions were set as described by Migues *et al.* (Migues et al., 2018). The mass spectrometry data were acquired in the negative ionization mode. The MS^n was carried out in automatic mode on the most abundant fragment ion in MS^n $(M–H)^-$.

2.4. Quantification of phenolic compounds

Twenty microliters of each sample were injected into a reversed-phase HPLC–DAD system (Agilent 1100). Compounds were separated on a Luna C18 column (Phenomenex, Macclesfield, UK). The mobile phase consisted of water/formic acid (99:1, v/v) and acetonitrile, delivered at a flow rate of 0.8 mL min^{-1} using a linear gradient. Individual compounds were tentatively identified based on their characteristic UV–Vis spectra and retention times (RT), and by comparison with peaks previously assigned in the HPLC–DAD–ESI/MS^n analysis. Chlorogenic acid (Merck, CAS 327–97–9) and rutin (Merck, CAS 153–18–4) were used as analytical standards. Compounds identified as cinnamoyl acid derivatives (Cinn-der) were quantified as chlorogenic acid at 320 nm, while flavonoid derivatives were quantified as rutin at 360 nm. Three replicates per sample were analyzed, and results were expressed as mg per g of freeze-dried weight (mg/g DW).

2.5. Volatile profiling and antifungal activity

Essential oils (EOs) and hydrolats were obtained from *A. prolifera* samples via hydrodistillation. Volatile profiles were analyzed using an Agilent 7890B gas chromatograph (Agilent Technologies, California, USA) equipped with an HP-5MS UI column and coupled to an Agilent 5977 A mass spectrometer. The oven temperature program started at 60 °C, increased to 250 °C at 3 °C/min, and then to 310 °C at 15 °C/min. The injector temperature was set at 250 °C. A 1 μL aliquot was injected in split mode (1:10). The mass spectrometer was operated in scan mode over a mass range of 50–550 *m/z*. Volatiles were identified by comparison with the NIST 2011 mass spectral library. For GC–MS analysis, a mixture of 10 μL of each EO and 990 μL of 9:1 hexane:ethyl acetate was prepared.

Antifungal activity of EOs and hydrolats was evaluated against nine plant fungal strains from the American Type Culture Collection (ATCC) and CEREMIC Culture Collection (CCC, Facultad de Ciencias Bioquímicas y Farmacéuticas, Universidad Nacional de Rosario, Argentina): *Botrytis cinerea* CCC 100–2017, *Penicillium citrinum* CCC 189–2001, *Fusarium graminearum* CCC 327–10, *F. oxysporum* CCC 186–06, *F. solanii* CCC 103–11, *F. semitectum* CCC 231–01, *Aspergillus flavus* ATCC 9170, *A. niger* ATCC 9029, and *A. fumigatus* ATCC 26934. Fungi were cultured on Potato Dextrose Agar (PDA) to induce conidiation and incubated at 28 °C for 3–10 days, depending on the species. Conidia were harvested by adding sterile physiological saline solution containing 0.01% Tween 80 to the colony surface and gently scraping with a sterile loop to release the spores. The resulting suspension was filtered through sterile gauze to remove hyphal fragments. The concentration of conidia was determined using a Neubauer hemocytometer, and the inoculum was adjusted to 5×10^4 CFU/mL with sterile saline solution in accordance with CLSI guidelines for filamentous fungi (Clinical and Laboratory Standards Institute CLSI, 2017).

Minimum inhibitory concentrations (MICs) were determined using the broth microdilution method in flat-bottom 96-well microplates (Greiner Bio-One, Wemmel, Belgium) following CLSI guidelines (Perczak et al., 2019; Ru et al., 2025). Stock solutions of EOs were prepared at 50 mg/mL in dimethyl sulfoxide (DMSO), while hydrolats were tested without dilution. Working solutions of EOs were obtained by serial dilution in culture medium to a concentration range of 1000–7.8 μg/mL, with a final DMSO concentration $\leq 1\%$ in all wells. Hydrolats were tested in a concentration range of 25–0.2% v/v. A volume of 100 μL of each test solution was added to the wells, followed by 100 μL of the fungal inoculum. Control wells included: growth control (medium with inoculum, no sample), sterility control (medium without

sample and inoculum replaced by sterile distilled water), and sample control (medium with sample and sterile distilled water instead of inoculum). Microplates were incubated at 28–30 °C under humid conditions without shaking during the species-specific time. The MIC was determined by visual assessment and defined as the lowest concentration at which complete (100%) inhibition of visible fungal growth was observed in comparison with the untreated control. Carbendazim (Carbendaglex, Buenos Aires, Argentina) was used as a positive control.

Minimum fungicidal concentrations (MFCs) were determined by plating 10 µL aliquots from MIC wells without visible growth onto Sabouraud dextrose agar (SDA), followed by incubation at 28 °C for species-specific durations. MFC was defined as the lowest concentration at which no fungal growth occurred. All assays were performed in duplicate.

2.6. Data analysis

An exploratory data assessment was performed using Principal Component Analysis (PCA) to visualize variation in (poly)phenolic and volatile compounds and to identify the variables that contributed most to sample variation. Differences in compound concentrations among samples were statistically tested at $p\text{-}value < 0.05$. First, normality and homogeneity of variance were assessed using the Shapiro–Wilk and Levene tests, respectively. When both assumptions were met, parametric tests (Analysis of Variance [ANOVA] followed by the Least Significant Difference [LSD] test) were performed. For variables that were not normally distributed, non-parametric tests (Kruskal–Wallis followed by Wilcoxon post-hoc test) were applied. All data analyses were performed in R (R Core Team, 2021).

3. Results

3.1. Identification of phenolic compounds

A total of 31 phenolic compounds were detected at 340 nm by HPLC-DAD in the *A. prolifera* organic extracts and most of them were present in all studied phenological stages and natural populations (Fig. 1 and Table 1). Among them, ten were identified as cinnamoyl acid -type compounds (**2-6**, **8**, **11**, **24**, **27** and **30** peaks), 19 as glycosylated flavonoids (**7**, **9**, **10**, **12**, **13-23**, **25**, **26**, **28** and **29** peaks) and two eluents could not be identified (**1**, **31**).

3.1.1. Cinnamoyl acid derivatives

Ten peaks (**2–6**, **8**, **11**, **24**, **27** and **30**) showed UV spectra of cinnamoyl acid derivatives (UV ~298sh, 326 nm). In particular, the peaks **2**, **3** and **5** showed the deprotonated molecular ion of *caffeoyl-quinic acid* (CQA) (*m/z* 353), **8** and **11** of *feruloyl-quinic acid* (FQA) (*m/z* 367), and **24** and **27** of *dicaffeoyl-quinic acid* (diCQA) (*m/z* 515). Considering the

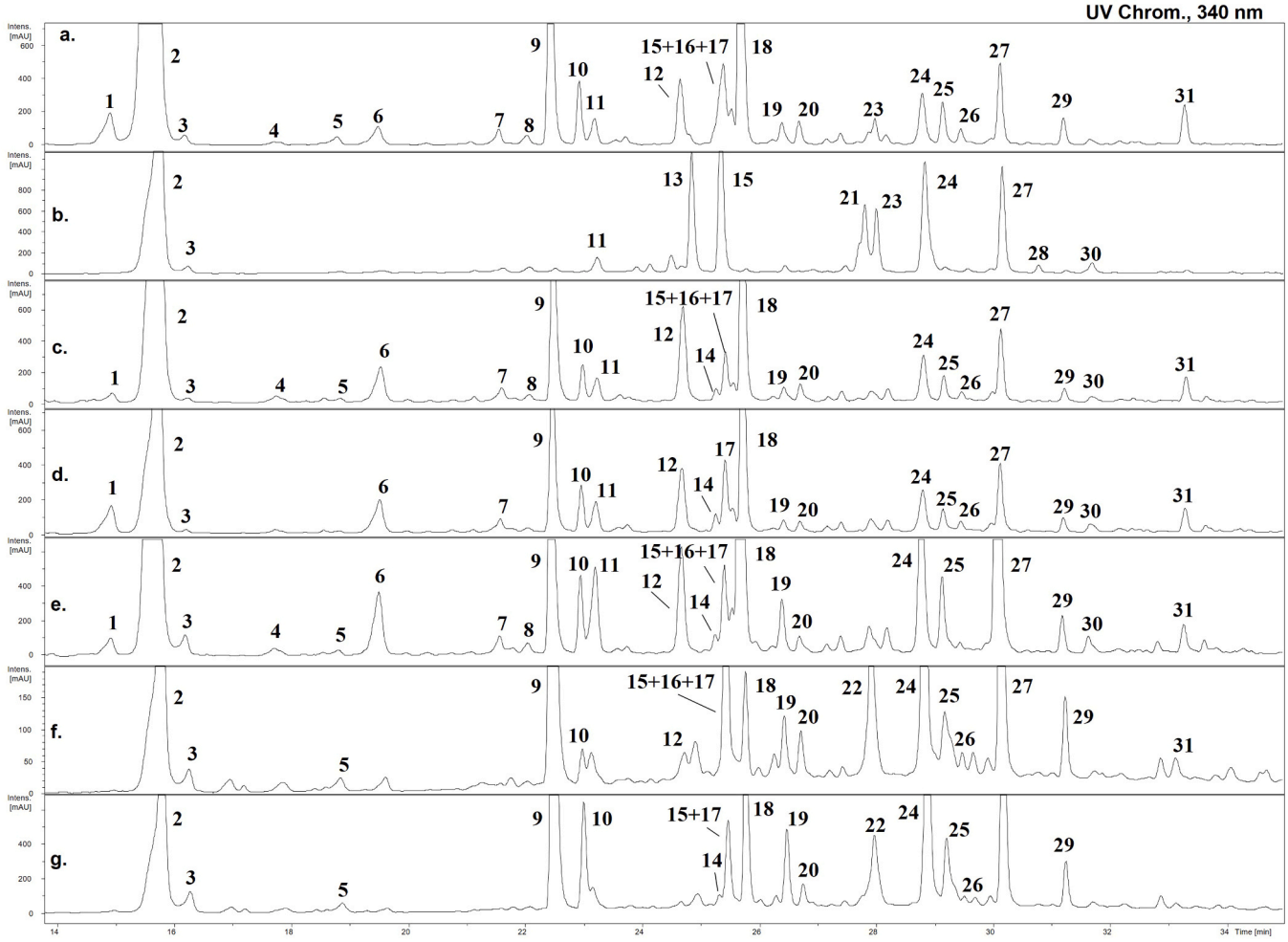

Fig. 1. Chromatographic profile of *A. prolifera* by HPLC-DAD at 340 nm in different plant material: **a.** C_Veg: sample from 41°08'S - 71°08'W at the vegetative stage; **b.** N_Flb: sample from 39°53'S - 70°42'W at the floral button stage; **c.** E_Flb: sample from 41°05'S - 70°49'W at the floral button stage, **d.** N_Flw: sample from 39°53'S - 70°42'W at flowering stage; **e.** E_Flw: sample from 41°05'S - 70°49'W at flowering stage; **f.** N_seeds: seeds from 39°53'S - 70°42'W; **g.** E_seeds: seeds from 41°05'S - 70°49'W. Full information of plant material's ID are detailed in Table 1. Numbers correspond to each identified polyphenol compound, and the identity of each one are detailed in Table 1.

Table 2
Content (mg/ g DW) of main identified (poly)phenolic compounds in *A. prolifera* organic extract.

Different provenances of plant material																		
ID	**Sampling Location**	**2**	**6**	**11**	**24**	**27**	**30**	**9**	**10**	**13**	**12**	**18**	**19**	**22**	**25**	**29**	**Tot Cinn**	**Tot Flav**
N	39°53'S - 70°42'W	11.84 ± 3.43 a	0.07 ± 0.07 b	0.10 ± 0.10 b	2.83 ± 1.09 A	2.53 ± 0.72 A	0.20 ± 0.15 b	0.23 ± 0.23 a	n.d.	2.84 ± 1.05	4.35 ± 1.27 A	0.31 ± 0.09 b	0.90 ± 0.78 A	n.d.	1.99 ± 0.20 A	n.d.	18.29 ± 5.02 b	11.07 ± 3.46 a
C	41°08'S - 71°08'W	14.86 ± 1.82 a	0.52 ± 0.13 b	1.06 ± 0.24 a	1.14 ± 0.16 A	2.30 ± 0.38 A	0.06 ± 0.03 c	5.21 ± 0.40 a	1.36 ± 0.36 A	n.d.	3.58 ± 1.60 A	6.61 ± 0.57 a	0.13 ± 0.08 A	n.d.	1.73 ± 0.81 A	n.d.	25.27 ± 1.97 ab	19.64 ± 2.14 a
E	41°05'S - 70°49'W	17.54 ± 0.68 a	1.48 ± 0.17 a	1.55 ± 0.17 a	2.01 ± 0.51 A	4.25 ± 1.19 A	0.31 ± 0.11 a	5.07 ± 0.96 a	1.93 ± 0.82 A	n.d.	0.71 ± 0.27 A	7.98 ± 1.06 a	0.13 ± 0.06 A	0.19 ± 0.19	0.66 ± 0.24 A	0.10 ± 0.10	31.63 ± 2.57 a	17.45 ± 2.24 a
Different phenological stages of plant material																		
ID	**Phenological Stage**	**2**	**6**	**11**	**24**	**27**	**30**	**9**	**10**	**13**	**12**	**18**	**19**	**22**	**25**	**29**	**Tot Cinn**	**Tot Flav**
Veg	Vegetative	12.93 ± 3.34 ab	0.21 ± 0.04 A	0.62 ± 0.05 A	1.35 ± 0.31 A	1.83 ± 0.18 a	n.d.	5.02 ± 0.34 b	0.88 ± 0.44 ab	n.d.	6.58 ± 2.50 A	6.00 ± 0.90 ab	n.d.	n.d.	3.13 ± 1.41 a	n.d.	23.09 ± 0.62 ab	23.25 ± 2.45 a
Flb	Flower bud	15.12 ± 2.15 a	0.63 ± 0.27 A	0.83 ± 0.34 A	2.15 ± 0.59 A	3.01 ± 0.59 a	0.25 ± 0.13 A	2.67 ± 1.10 b	0.52 ± 0.23 b	1.42 ± 0.79	2.27 ± 1.09 A	3.26 ± 1.40 b	0.48 ± 0.40 a	n.d.	1.10 ± 0.41 b	0.10 ± 0.10 B	24.06 ± 3.56 ab	12.16 ± 1.75 b
Flw	Flowering	16.74 ± 1.1 a	1.31 ± 0.22 A	1.52 ± 0.24 A	1.74 ± 0.56 A	3.89 ± 1.22 a	0.23 ± 0.07 A	5.22 ± 1.04 b	2.33 ± 0.80 a	n.d.	0.90 ± 0.20 A	8.48 ± 0.86 a	0.23 ± 0.08 a	0.19 ± 0.19 a	0.72 ± 0.21 b	n.d.	30.43 ± 3.23 a	18.84 ± 2.07 a
Seeds	Seeds	6.30 ± 1.82 b	n.d.	n.d.	4.16 ± 1.34 A	3.24 ± 1.36 a	n.d.	8.99 ± 1.24 a	1.31 ± 0.75 ab	n.d.	n.d.	3.57 ± 1.52 b	0.18 ± 0.11 a	0.67 ± 0.20 b	0.17 ± 0.17 b	0.61 ± 0.18 A	16.30 ± 4.99 b	15.51 ± 3.88 ab

Numbers in the column label correspond to the compound ID in Table 1. Tot Cinn: total of cinnamic acid derivatives. Tot Flav: total of flavonoid derivatives

relative abundance of their ions from MS fragmentations (Table 2), these compounds were identified as 5-CQA (2), 5-CQA isomer (5), 4-CQA (3), 5-FQA (8), 4-FQA (11), 3,5-diCQA (24) and 3,4-diCQA (27) (Table 2). The peak **4** exhibited [M-H]- ion at *m/z* 341 and a loss of 162 and 204 (162 + 42) amu fragments (hexosyl and acetylhexosyl radicals) in MS2; thus, it was identified as *caffeoyl-hexoside*. The peak **6** exhibited [M-H]- ionat *m/z* 797 and was identified as caffeoylquinic acid derivative since there was a loos of hexosyl radical in the MS fragmentation, which resulted in a base peak at *m/z* 635, and also the presence of ions 353 (CQA-H) and 191 (QA-H) in MS3 (797→635) among others (Table 2). The deprotonated molecular ion of compound **30** (*m/z* 601) showed fragment losses of 44 and 86 amu in MS2 fragmentation that indicated a malonyl radical (Table2). The (MS3[601→515]-) fragmentation (Table 2), confirmed that compound **30** is a *malonyl-dicaffeoylquinic acid*.

3.1.2. Flavonoid derivatives

3.1.2.1. Flavonoid-O-monoglycosides. The compounds **12** and **16** showed UV spectra of flavanons and **19** and **25** ions of flavonol-3-O-sustituted and deprotonated molecular ions of mono-glycosides (Table 2). In MS fragmentation of these compounds, it were identified as base peaks the ions of their deprotonated aglycones (aglyc-H/2H): 287 amu (**12** and **16**, tetrahydoxyflavanone, eriodictyol), 301 amu (**19**, 3,5,7,3 ',4 '-pentahydroxyflavone, quercetin) and 314 amu (**25**, 3,5,7,4 '-tetrahydroxy-3 '-methoxyflavone, isorhamnetin) and loses of 162 amu. The radicals of 162 amu could be either by a -caffeoyl or a -hexosyl. However, compounds **19** and **25** showed a band at 220/230 nm of a hexosyl radical in the UV spectra, while in compounds **12** and **16** appeared a band at 330 nm with low intensity which is not typical expected for an acetylation with caffeic acid. Therefore, these compounds were namely as: *erioditoyl-O-hexosyde* (**12** and **16**), *quercetin-3-O-hexosyde* (**19**) and *isorhamnetin-3-O-hexosyde* (**25**). Peaks **22** and **29** showed the deprotonated molecular ions 42 amu higher than **19** and **25** and the same aglycones, respectively; therefore, these compounds were considered as acetyl derivatives. Besides, the low abundance of ion [(M-H)-42]- in **22** and its lack in **29** indicated that the acetylation was located at 6 position of hexose and, thus, these were named as *quercetin-3-O-(6-acetyl) hexosyde* (**22**) and *isorhamnetin-3-O-(6-acetyl) hexosyde* (**29**).

3.1.2.2. Flavonoid-O-diglycosides. The compounds **10**, **13**–**15**, **18** and **23** showed UV spectra of flavonoid-3-O-sustituted (flavonols) and deprotonated molecular ions of di-glycosides (Table 2). In the MS fragmentation pattern of these compounds, it was observed (as base peak) thosecorresponding with their deprotonated aglycones: 301 amu, quercetin (**10**, **13** and **15**); 285 amu, kaempferol (**14**); and 315 amu, isorhamnetin (**18** and **23**). Additionally, the absence of other ions (products of a cleavage of interglycosidic linkages) indicating that these compounds were glycosyl(1→6)glycosides: hexosyl(1→6) hexosydes (**10**, **14** and **18**), rhamnosyl(1→6) hexosydes (**15** and **23**), and pentosyl (1→6) hexosyde (**13**). Therefore, the compounds were identified as: *quercetin-3-O-gentobioside* (**10**), *quercetin-3-O-pentosyl (1→6) hexosyde* (**13**), *kaempferol-3-O-gentobioside* (**14**), *quercetin-3-O-rutinoside* (**15**), *isorhamnetin-3-O-gentobioside* (**18**) and *isorhamnetin-3-O-rutinoside* (**23**).

3.1.2.3. Flavonoid-C-glycosides. The compounds **9** and **17** with deprotonated molecular ions at *m/z* 447 and 431 showed in MS^2 fragmentations losses of −90 and −120 amu (357/327 and 341/311, respectively), indicating a C-hexosylation. These ions ([M-H)-90/-120]-) in mono-C-glycosylflavones corresponded with Aglycone + 71/+ 41, which characterized the aglycon of peak **9** as tetrahydroxyflavon (*m/z* 286) and of peak **17** as trihydroxyflavon (*m/z* 270). The UV spectrum of compound **9** not fully coincided with luteolin and the great abundance of −90 amu together with the presence of ion (M-H)-18 could indicate the glycosylation in 6-C position. Therefore, this compound was identified as *tetrahydroxyflavon-6-C-hexoside* (Table 2). The UV spectrum of compound **17** is coincident with apigenin and the relative abundance of the ions of its fragmentation (-18/-90) indicated an 8-C-glycosylation; therefore, this compound was named as *apigenin-8-C-hexoside* (Table 2). The compounds **20** and **26** showed deprotonated molecular ions 42 amu higher than **9** and **17** (*m/z* 489/473), which indicated an extra acetylation. The ions of their fragmentations were like **9** and **17**, but the losses were 42 amu higher (M-H)- (42 +18)/-(42 +90/-(42 +120) (Table 2). The losses of radical and fragments caused by internal breakage of their hexose (42 +90/42 +120) suggested that the acetylation is located at position 6 of their hexose (hard cleavage). Therefore, these compounds were named as: *tetrahydroxyflavon-6-C-(6-acetyl) hexoside* (**20**) and *apigenin-8-C-(6-acetyl) hexoside* (**26**) (Table 2).

3.1.2.4. Other Flavonoids. The compound **7** showed the deprotonated molecular ions 206 amu higher to the one of peak **29**, which could indicate a sinapoyl derivative. The MS3 (729→519) was like the MS2 of **29** and thus, it was named as *Sinapoyl-Isorhamnetin(acetyl) hexoside*. The compounds **21** and **28** had deprotonated molecular ions at *m/z* 607 and 621, respectively, and they differed in 14 amu and by the ions in their MS fragmentations (Table 2). Ions at *m/z* 463 and 301 were observed in **21** and 477 and 315 in **28** and, thus, they were identified as *quercetin-3-O-hexosyl derivative* (**21**) and *isorhamnetin-3-O-hexosyl derivative* (**28**).

Some qualitative differences were found among the plant materials studied (Table 2). *Quercetin-3-O-(acetyl) hexoside* (**22**) was only present in seeds, while the compounds **4**, **6**, **7**, **8**, **11**, **13**, **21**, **23**, **28**, and **30** were absent in this material. In addition, differences in (poly)phenolic profiling were found among the analyzed phenological stages of the aerial part (Table 2). In example, *kaempferol-3-O-gentiobioside* (**14**) and *malonyl-diCQA* (**30**) were present in reproductive stages but absent in vegetative ones. *A. prolifera* provenances also showed qualitative differences in the (poly)phenol profile. The northern population at the floral button (N_Flb) stage was the sample that most qualitatively differed from the remaining ones (Fig. 1, Table 1). *Quercetin-3-O-(6-pentosyl) hexoside* (**13**), *quercetin-3-O-hexosyl derivatives* (**21**) and *isorhamnetin-3-O-hexosyl derivatives* (**28**) were only present in N_Flb; whereas compounds **4**, **5**, **6**, **7**, **9**, **10**, **12**, **14**, **16**, **17**, **18**, **19**, **20**, **22**, **25**, **26**, **28**, and **29** were absent. Regarding (poly)phenol profile in seeds, differences in C and E provenances were found. Eriodyctiol derivatives (**12** and **14** compounds) were only present in the western population (C) and *kaempferol-3-O-gentiobioside* was only present in the eastern one (E).

3.2. Quantification of phenolic compounds

On average, *A. prolifera* extracts contained 4.1 (±1.4) g of polyphenols per 100 g of dry weight, comprising 2.4 (± 0.9) g of cinnamoyl acid derivatives (Cinn-der) and 1.7 (± 0.6) g of flavonoid-type compounds (Flav). Quantification of major cinnamoyl acid derivatives and flavonoid-type compounds is provided in Table 2. 5-caffeoyl quinic acid (5-CQA) represented the predominant compound, accounting for ~55–65% of total cinnamoyl acid derivatives. Eriodictyol-hexoside (Eridct-hex), isorhamnetin-3-O-gentiobioside (Isorh-3-O-gentiob), and a tetrahydroxyflavone-type compound constituted the main constituents of the flavonoid fraction.

Principal component analysis (PCA) accounted for more than 62% of the total (poly)phenolic variation within the first two components (Fig. 2). Individual compounds contributed less than 8% each, and several metabolites exhibited positive correlations. Discriminant analysis indicated that seeds were clearly distinct from vegetative and flowering aerial parts (Fig. 2a). Additionally, the northern population (N) stood apart from the other provenances (Fig. 2b).

Significant differences in total Cinn-der content were found among the studied populations, whereas no notable differences were observed for total flavonoid derivatives (Table 2). Total Cinn-der concentrations

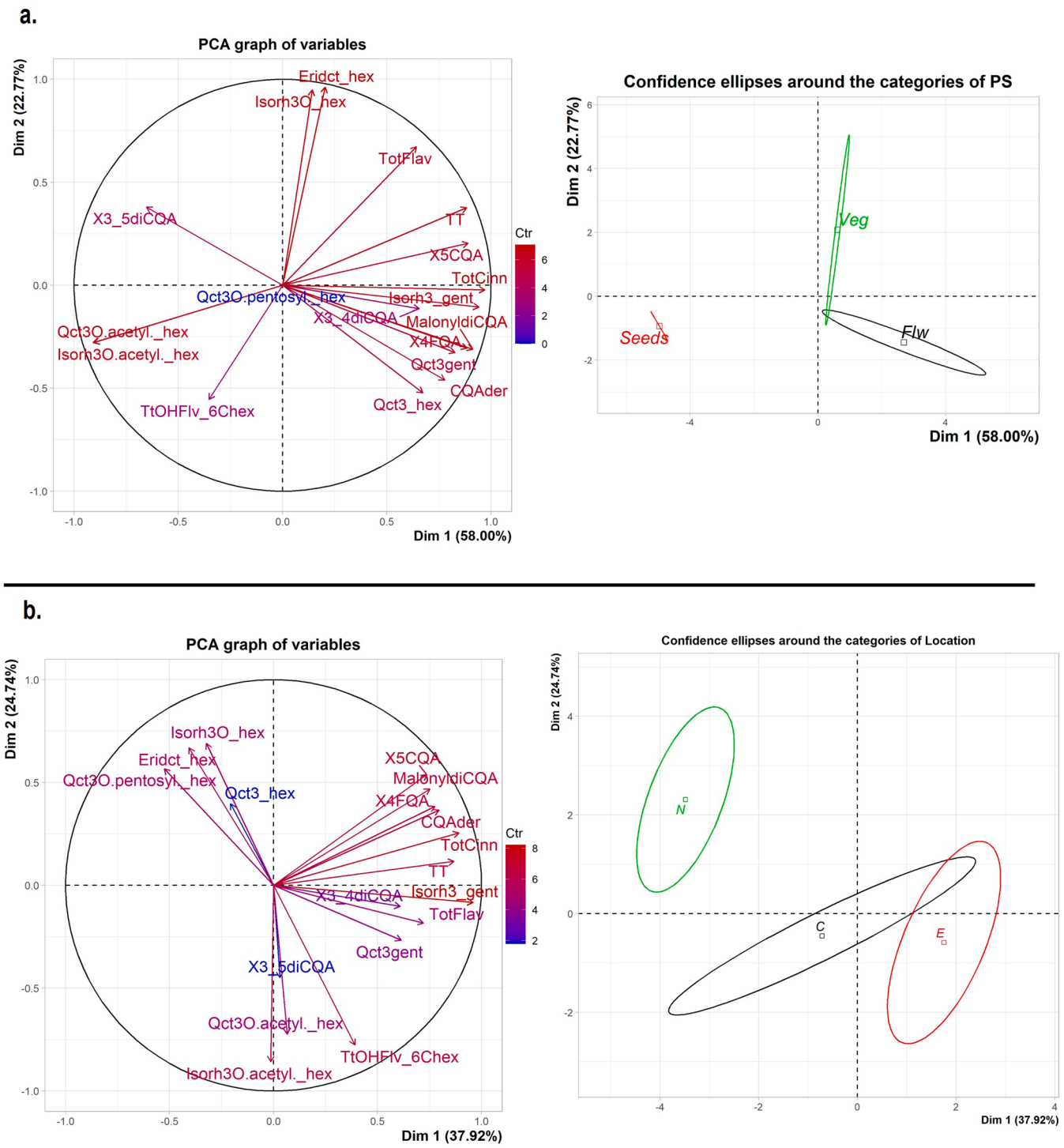

Fig. 2. Principal Components Analysis of secondary metabolic profiling in *A. prolifera* when different phenological stages (**a**) and provenances (**b**) of plant material are considered.

ranged from 18.29 (± 8.69) mg/g DW in the northern population (N) to 31.63 (± 6.28) mg/g DW in the eastern population (E), while flavonoid derivatives varied from 11.07 (± 5.99) mg/g DW in N to 17.45 (± 5.47) mg/g DW in E. Considering phenological stages, significant differences were found in both Cinn-der and Flav compounds. Specifically, 5-CQA, CQA derivatives, and 4FQA attained their highest levels at flowering. Regarding the flavonoid fraction, Eridct-hex and Isorh-3-O-hexoside were more concentrated at flowering, whereas Isorh-3-O-gentiobioside content was higher at the vegetative stage.

3.3. Essential oil composition and their antifungal activity

A total of fifty-five different volatile compounds were detected in *A. prolifera* essential oils, of which 51 were properly identified by GC-MS and 4 compounds remained unknown (Suppl. Mat. 1). Among volatiles, D-limonene, terpinen-4-ol, aromandendrene, α-muurolene, spathulenol, δ-cadinene, γ-cadinene, T-muurolol and α-cadinol, and one non-identified volatile (*unknown 4*) were present across all samples. However, the relative proportions of these shared compounds were variable among samples. PCA analysis showed that most compounds contributed

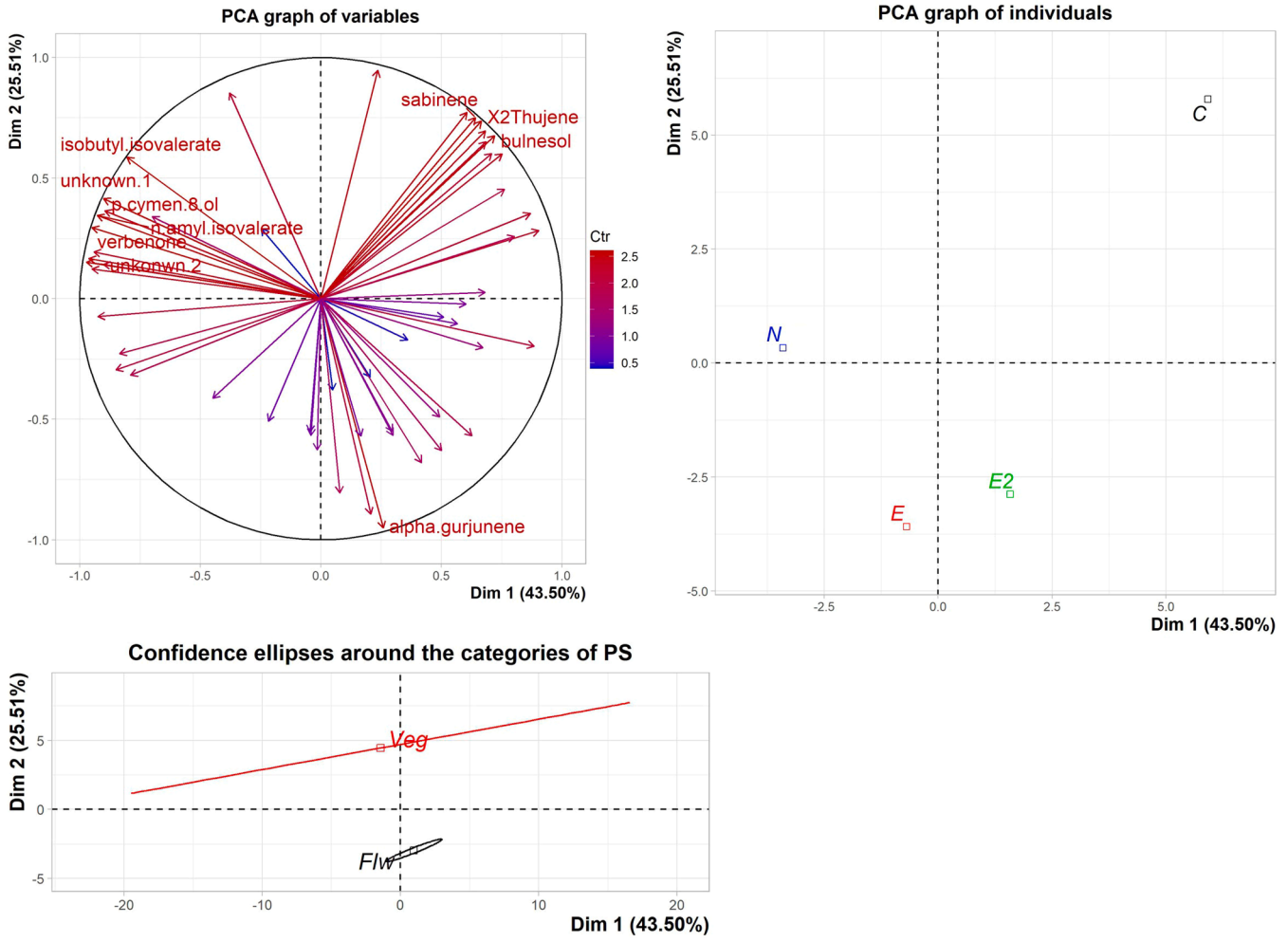

Fig. 3. Principal Components Analysis of essential oil profile in *A. prolifera* when different provenances and phenological stages of plant material are considered.

Table 3
In vitro antifungal evaluation of essential oils (tested concentration ≤ 1000 μg/mL) and hydrolats of *A. prolifera* against filamentous fungi.

Essential oils	MIC/MFC (μg/mL)								
	Afu[a]	***An***[b]	***Afl***[c]	***Bc***[d]	***Pc***[e]	***Fg***[f]	***Fo***[g]	***Fse***[h]	***Fso***[i]
C_Veg	i	i	i	i	i	250/250	i	i	i
N_Veg	i	i	i	i	i	250/250	i	i	i
E_Flw	i	i	i	i	i	500/500	i	i	i
E2_Flw	i	i	i	i	i	250/250	i	i	i
N_Flw	i	i	i	i	i	250/250	i	i	i
Hidrolats	**MIC/MFC (% v/v)**								
	Afu[a]	***An***[b]	***Afl***[c]	***Bc***[d]	***Pc***[e]	***Fg***[f]	***Fo***[g]	***Fse***[h]	***Fso***[i]
C_Veg	25/i	i	i	25/i	i	i	i	i	i
N_Veg	i	i	i	i	i	i	i	i	i
E_Flw	i	i	i	i	i	i	i	i	i
E2_Flw	i	i	i	i	i	i	i	i	i
N_Flw	i	i	i	i	i	i	i	i	i
CBZ	4	4	4	62.5	4	4	4	4	4

CBZ: Carbendazim; i: inactivity
[a]Aspergillus fumigatus ATCC 26934; [b]A. niger ATCC 9029; [c]A. flavus ATCC 9170; [d]Botrytis cinerea CCC 100–2017; [e]Penicillium citrinum CCC 189–2001; [f]Fusarium graminearum CCC 327–10; [g]F. oxysporum CCC 186–06; [h]F. semitectum CCC 231–01; [i]F. solanii CCC 103–11
C_Veg: sample from 41°08's - 71°08'W at the vegetative stage; N_Veg: sample from 39°53's - 70°42'W at the vegetative stage; E_Flw: sample from 41°05's - 70°49'W at the flowering stage; E2_Flw: sample from 40º53's-68º3'W at flowering stage; N_Flw: sample from 39°53's - 70°42'W at flowering stage.

slightly to the differentiation of EO profiling. In addition, differences in the volatile relative concentration were detected among phenological stages and provenances of plant materials (Fig. 3).

Antifungal assays indicated differential susceptibility of the tested fungal species to *A. prolifera* extracts (Table 3). Only *F. graminearum* was inhibited by EOs at concentrations below 1000 μg/mL. Moreover, MIC

and MFC values ranged between 500 and 250 μg/mL among the EO samples. Regarding hydrolats, only the C_Veg sample exhibited antifungal activity, with a MIC of 25% v/v against *A. fumigatus* and *B. cinerea* (Table 3), although no fungicidal effect was observed.

4. Discussion

Consistent with its adaptation to harsh growing conditions, the extremely resilient shrub *A. prolifera* exhibited a rich secondary metabolite profile, highlighting its potential as a source of bioactive compounds for natural product development. Metabolic changes during plant growth were evident from the variability in secondary metabolite composition across the phenological stages studied. In addition, both qualitative and quantitative differences were observed among natural populations. Secondary metabolite production and accumulation play a key role in plant adaptation to abiotic and biotic stresses (You and Chan, 2015; Adhikary and Dasgupta, 2023). In particular, antioxidant compounds are essential for maintaining reactive oxygen species (ROS) at non-toxic intracellular levels (Foyer and Noctor, 2005). Furthermore, volatile compounds are crucial components of plant defense against herbivores and pathogens (Hu et al., 2021). Natural variability in the chemical profile of a species may arise from interactions between phenological stage and local environmental conditions (Petrén et al., 2024).

Previous work on *A. prolifera* has characterized root decoctions, revealing a rich polyphenol mixture with antioxidant and anti-glycemic properties (Ru et al., 2025). Comparison between the root (previous study) and aerial parts (current study) indicate tissue-specific metabolic diversity, with the aerial parts exhibiting higher total polyphenol content than the roots. Regarding essential oil composition, earlier studies reported only resin acids, α- and β-pinene, limonene, and two mulinane diterpenoid acids (Nicoletti et al., 1996). Our results indicate a more complex and enriched volatilome. It is important to note that previous studies related to the chemical composition of *A. prolifera* only have considered one provenance of plant material (Nicoletti et al., 1996; Echenique et al., 2014; Berruezo et al., 2022). Our findings suggest that both the origin and the developmental stage of plant material strongly influence *A. prolifera* chemical composition.

This study reports, for the first time, the antifungal activity *in vitro* of *A. prolifera* EOs and hydrolats. Antifungal efficacy varied among the tested fungal species. Notably, *A. prolifera* EOs showed marked activity against *F. graminearum*, a major cereal pathogen that has developed a high level of resistance to the most widely used fungicides. A concentration of 250 μg/mL (~ 0.278 μL/mL) of most EO samples inhibited 100% mycelial growth and exhibited fungicide effects. Several plant-essential oils have been shown to successfully inhibit this pathogen mycelial growth (Perczak et al., 2019; Ru et al., 2025; Seepe et al., 2021; Harčárová et al., 2021). Among them, *Cinnamomum zeylanicum* (cinnamon bark), *Foeniculum vulgare* (fennel seeds), *Origanum vulgare* (oregano herb), *Syzygium aromaticum* (clove), *Thymus hiemalis* (verbena leaves and flowers), and *Thymus vulgaris* (thyme leaves) have been reported to induce a total inhibition of *F. graminearum* mycelial growth at concentration below 0.8 μL/mL (~720 μg/mL). Compared with these EOs, most *A. prolifera* samples performed nearly twice as effectively. While the *in vitro* fungicidal activity of *A. prolifera* EOs is promising, validation under agricultural field conditions remains necessary. Furthermore, evaluating the stability of the bioactive molecules and identifying the most effective application strategies will be crucial for optimizing formulations and ensuring their efficient practical implementation.

Intra-species variability in antifungal activity against *F. graminearum* has been reported for *Cinnamomum camphora*, where MICs ranged from 12.8 μL/mL in fresh leaf EO to 3.2 μL/mL in senescent leaf EO (Ru et al., 2025). These observations agree with our findings, emphasizing the importance of assessing natural chemical variability when selecting superior plant material for biopesticide development. Comparative analysis of essential oil (EO) profiles from samples exhibiting higher and lower antifungal activity enables the identification of compositional patterns underlying variability in efficacy. The superior antifungal activity against *Fusarium graminearum* observed in EOs from N_Veg and E2_Flw relative to E_Flw can be primarily attributed to their higher abundance of the oxygenated monoterpenoids terpinen-4-ol and α-terpineol, which exert antifungal effects by disrupting fungal cell membrane integrity through alterations in lipid bilayer fluidity and inhibition of ergosterol biosynthesis (Kong et al., 2019). Meanwhile, the higher contents of D-limonene and α-pinene in C_Veg (11.0% and 8.2%, respectively) and N_Flw (44.4% and 19.5%, respectively) compared with E_Flw (2.3% and 1.1%, respectively) likely contribute to their superior antifungal efficacy against *F. graminearum*, as both monoterpenes have been reported to exhibit strong inhibitory activity against *Fusarium* spp (Jaramillo-Colorado et al., 2025). D-limonene induces membrane damage, disrupts ribosomal function and alters mitochondrial biosynthesis in *F. proliferatum* (Zhou et al., 2025). In contrast, although there is evidence that α-pinene exhibits inhibitory effect on Fusarium spp. mycelial growth (Jaramillo-Colorado et al., 2025), its antifungal mechanism of action remains poorly understood. Collectively, these compositional features and their associated synergistic interactions likely underlie the superior antifungal activity of C_Veg, N_Veg, E2_Flw, and N_Flw relative to E_Flw. Further investigation into the activity of individual compounds against *F. graminearum* is warranted to verify this hypothesis. Additionally, hydrolats from the population located at 41°08's–71°08'W represent valuable byproducts of EO extraction, since they exhibited fungistatic effects against *A. fumigatus* and *B. cinerea*. Therefore, this plant material is suggested as a promising and valuable option for antifungal biocontrol applications. Although *A. prolifera* is a widely distributed native shrub with high invasive capacity (de Torres Curth et al., 2020), efforts should focus on the sustainable harvesting or domestication of this species to enable the environmentally responsible production of biofungicides. Notably, Troncoso et al (Troncoso et al., 2020). established an efficient propagation methodology for *Azorella* spp. under controlled conditions, providing a useful tool and feasible framework for this purpose.

Overall, this study highlights the potential of *A. prolifera* EOs for controlling *F. graminearum* pathogen. Furthermore, it underscores the relevance of considering natural variability in the species' chemical profile when selecting plant material with superior antifungal activity. The enhanced efficacy appears to be associated with the higher relative abundance of oxygenated monoterpenoids, such as terpinen-4-ol and α-terpineol, as well as other key compounds, including D-limonene and α-pinene. Notably, samples from the 41°08's–71°08'W population are particularly promising, not only due to their high efficacy against *F. graminearum*, but also because of their complementary antifungal activity against *A. fumigatus* and *B. cinerea*.

Funding

This work was supported by the Agencia Nacional de Promoción Científica y Tecnológica (Grant numbers PICT-2020-SERIEA-03159, PICT-2020-SERIEA-02687), CONICET (Grant number PIBBA 0287), Universidad Nacional de Rosario (Grant number 80020210300027UR) and R&D Agreement INTA EEA Bariloche-HC. This work was also partially supported by 'GYPSME' project Ref. PID2024–159400NB-I00 funded by MICIU/AEI /10.13039/501100011033 and by ERDF (European Regional Development Fund), European Union (EU).

CRediT authorship contribution statement

Mattera Maria Gabriela: Writing – original draft, Visualization, Resources, Project administration, Investigation, Funding acquisition, Formal analysis, Data curation, Conceptualization. **Estefanía Butassi:** Writing – review & editing, Resources, Investigation, Funding acquisition, Formal analysis. **Federico Ferreres:** Writing – review & editing, Formal analysis. **Melina Di Liberto:** Writing – review & editing,

Resources, Investigation, Formal analysis. **Mónica Hourcade:** Writing – review & editing, Formal analysis. **Laura Svetaz:** Writing – review & editing, Supervision, Resources, Investigation, Funding acquisition, Formal analysis. **Araceli Bader:** Writing – review & editing, Investigation. **Diego. A. Moreno:** Writing – review & editing, Validation, Supervision, Resources, Funding acquisition, Data curation.

Declaration of Competing Interest

The authors declare that they have no known competing financial interests or personal relationships that could have appeared to influence the work reported in this paper

Acknowledgments

the authors thank M. Battistelli, A. Mazzoni and G. Caballé for their assistance in material collection.

Plant material

M.G.M and colleagues that participate in plant collection undertook the formal identification of the plant material used in this study. A voucher specimen of this material has not been deposited in a public herbarium. Permissions to collect the aerial part of *A. prolifera* in the chosen sites were obtained from provincial governments when required.

Statements and Declarations

None.

Additional Material

Supplementary Material 1 Essential oil composition (%) in *A. prolifera* determined by GC-MS.

Appendix A. Supporting information

Supplementary data associated with this article can be found in the online version at doi:10.1016/j.napere.2026.100191.

Data availability

Data will be made available on request.

References

Tang, F.H.M., Wyckhuys, K.A.G., Li, Z., Maggi, F., Silva, V., 2025. Transboundary impacts of pesticide use in food production. Nat. Rev. Earth Environ. 6 (6). https://doi.org/10.1038/s43017-025-00673-y.

Aremu, A.O., Omogbene, T.O., Fadiji, T., Lawal, I.O., Opara, U.L., Fawole, O.A., 2024. Plants as an alternative to the use of chemicals for crop protection against biotic threats: trends and future perspectives. Eur. J. Plant Pathol. 170 (4). https://doi.org/10.1007/s10658-024-02924-y.

Carrasco-Puga, G., Díaz, F.P., Soto, D.C., Hernández-Castro, C., Contreras-López, O., Maldonado, A., Latorre, C., Gutiérrez, R.A., 2021. Revealing hidden plant diversity in arid environments. Ecography 44 (1). https://doi.org/10.1111/ecog.05100.

Eshel, G., Araus, V., Undurraga, S., Soto, D.C., Moraga, C., Montecinos, A., Moyano, T., Maldonado, J., iaz, Varala, F.P., Nelson, K., Contreras-Lopez, C.W., Pal-Gabor, O., Kraiser, H., Carrasco-Puga, T., Nilo-Poyanco, G., Zegar, R., Orellana, C.M., Montecino, A., M, Gutierrez, R.A., 2021. Plant ecological genomics at the limits of life in the Atacama Desert. Proc. Natl. Acad. Sci. USA 118 (46). https://doi.org/10.1073/pnas.2101177118.

You, J., Chan, Z., 2015. Ros regulation during abiotic stress responses in crop plants (Issue DEC). Front. Plant Sci. 6. https://doi.org/10.3389/fpls.2015.01092.

Adhikary, S., Dasgupta, N., 2023. Role of secondary metabolites in plant homeostasis during biotic stress. Biocatal. Agric. Biotechnol. 50, 102712. https://doi.org/10.1016/J.BCAB.2023.102712.

Petrén, H., Anaia, R.A., Aragam, K. sen, Bräutigam, A., Eckert, S., Heinen, R., Jakobs, R., Ojeda-Prieto, L., Popp, M., Sasidharan, R., Schnitzler, J.-P., Steppuhn, A., Thon, F. M., Unsicker, S.B., van Dam, N.M., Weisser, W.W., Wittmann, M.J., Yepes, S., Ziaja, D., Junker, R.R., 2024. Understanding the chemodiversity of plants: Quantification, variation and ecological function. Ecol. Monogr. 94 (4), e1635. https://doi.org/10.1002/ecm.1635.

Ferreyra, M., Ezcurra, C., 2022. In: Ferreyra, M.B., Ezcurra, C. (Eds.), Plants of Extra-Andean Patagonia. Patagnian Steppe and Southern Monte. Ediciones LBN (First edition).

Fernández, M., Ezcurra, C., Calviño, C.I., 2017. Species limits and morphometric and environmental variation within the South Andean and Patagonian *Mulinum spinosum* species-group (Apiaceae-Azorelloideae). Syst. Biodivers. 15 (5). https://doi.org/10.1080/14772000.2016.1273975.

Molares, S., Ladio, A., 2014. Medicinal plants in the cultural landscape of a Mapuche-Tehuelche community in arid Argentine Patagonia: An eco-sensorial approach. J. Ethnobiol. Ethnomed. 10 (1). https://doi.org/10.1186/1746-4269-10-61.

Estomba, D., Ladio, A., Lozada, M., 2006. Medicinal wild plant knowledge and gathering patterns in a Mapuche community from North-western Patagonia. J. Ethnopharmacol. 103 (1). https://doi.org/10.1016/j.jep.2005.07.015.

Sülsen, V., Güida, C., Coussio, J., Paveto, C., Muschietti, L., Martino, V., 2006. vitro evaluation of trypanocidal activity in plants used in Argentine traditional medicine. Parasitol. Res. 98 (4). https://doi.org/10.1007/s00436-005-0060-4.

Nicoletti, M., di Fabio, A., D'Andrea, A., Salvatore, G., van Baren, C., Coussio, J.D., 1996. Diterpenoid acids from *Mulinum spinosum*. Phytochemistry 43 (5). https://doi.org/10.1016/S0031-9422(96)00403-7.

Echenique, D., Chiaramello, A., Rossomando, P., Mattana, C., Alcaráz, L., Tonn, C., Laciar, A., Satorres, S., 2014. Antibacterial activity of *Mulinum spinosum* extracts against slime-producing *Staphylococcus aureus* and methicillin-resistant Staphylococcus aureus isolated from nasal carriers. Sci. World J. *2014*. https://doi.org/10.1155/2014/342143.

Gironés-Vilaplana, A., Mena, P., García-Viguera, C., Moreno, D.A., 2012. A novel beverage rich in antioxidant phenolics: Maqui berry (*Aristotelia chilensis*) and lemon juice. LWT 47 (2). https://doi.org/10.1016/j.lwt.2012.01.020.

Migues, I., Baenas, N., Gironés-Vilaplana, A., Cesio, M.V., Heinzen, H., Moreno, D.A., 2018. Phenolic profiling and antioxidant capacity of *Eugenia uniflora* L. (Pitanga) samples collected in different uruguayan locations. Foods 7 (5). https://doi.org/10.3390/foods7050067.

Clinical and Laboratory Standards Institute (CLSI), 2017. Reference method for broth dilution antifungal susceptibility testing of filamentous fungi, 3rd edn CLSI standard M38. Clinical and Laboratory Standards Institute, Wayne.

R Core Team. R: A language and environment for statistical computing. R Foundation for Statistical Computing, Vienna, Austria. 2021. URL ⟨https://www.R-project.org/⟩.

Foyer, C.H., Noctor, G., 2005. Redox homeostasis and antioxidant signaling: A metabolic interface between stress perception and physiological responses. Plant Cell 17 (7). https://doi.org/10.1105/tpc.105.033589.

Hu, L., Zhang, K., Wu, Z., Xu, J., Erb, M., 2021. Plant volatiles as regulators of plant defense and herbivore immunity: molecular mechanisms and unanswered questions. Curr. Opin. Insect Sci. 44, 82–88. https://doi.org/10.1016/J.COIS.2021.03.010.

Berruezo, S., Ferreyra, S., Fontana, A., de Paola, M., Pérez, M.B., Scapini, C., Cremer, C., Castro, C., 2022. *Mulinum spinosum* root extract, rich in antioxidant compounds, mitigates harmful effects in mice with diet-induced metabolic syndrome. Phytomedicine 2 (1). https://doi.org/10.1016/j.phyplu.2021.100169.

Perczak, A., Gwiazdowska, D., Marchwińska, K., Juś, K., Gwiazdowski, R., Waśkiewicz, A., 2019. Antifungal activity of selected essential oils against *Fusarium culmorum* and *F. graminearum* and their secondary metabolites in wheat seeds. Arch. Microbiol. 201 (8). https://doi.org/10.1007/s00203-019-01673-5.

Ru, Q., Huang, Y., Jin, Z., Yu, D., Fu, Z., Tian, J., Guo, M., Li, X., Yang, M., Luo, J., 2025. Antifungal activity and inhibitory mechanism of essential oil from fresh and fallen leaves of *Cinnamomum camphora* (L.) presl against zearalenone-producing *Fusarium graminearum*. LWT 231. https://doi.org/10.1016/j.lwt.2025.118331.

Seepe, H.A., Nxumalo, W., Amoo, S.O., 2021. Natural products from medicinal plants against phytopathogenic fusarium species: Current research endeavours, challenges and prospects. Molecules 26 (21). https://doi.org/10.3390/molecules26216539.

Harčárová, M., Čonková, E., Proškovcová, M., Váczi, P., Marcinčáková, D., Bujňák, L., 2021. Comparison of antifungal activity of selected essential oils against *Fusarium graminearum* in vitro. Ann. Agric. Environ. Med. 28 (3). https://doi.org/10.26444/aaem/137653.

Kong, Q., Zhang, L., An, P., Qi, J., Yu, X., Lu, J., Ren, X., 2019. Antifungal mechanisms of α-terpineol and terpene-4-alcohol as the critical components of *Melaleuca alternifolia* oil in the inhibition of rot disease caused by Aspergillus ochraceus in postharvest grapes. J. Appl. Microbiol. 126 (4), 1161–1174. https://doi.org/10.1111/jam.14193.

Jaramillo-Colorado, B.E., Arroyo-Salgado, B., Palacio-Herrera, F.M., 2025. Antifungal activity of four Piper genus essential oils against postharvest fungal *Fusarium* spp. isolated from *Mangifera indica* L. and *Persea americana* Mill. fruits. Ind. Crops Prod. 223. https://doi.org/10.1016/j.indcrop.2024.120170.

Zhou, S.W., Zhu, Y., Qin, X.J., Li, Y., Noiprasert, S., Apiwongsrichai, K., Xu, F.R., Liu, X. Y., Dong, X., 2025. D-limonene inhibits the growth of *Fusarium proliferatum* by decreasing H3K9ac and H3K27ac modifications. BMC Genom. 27 (1), 55. https://doi.org/10.1186/s12864-025-12389-w.

de Torres Curth, M., Ghermandi, L., Zimmerman, V., 2020. Living in a world of fire: the population dynamics of *Mulinum spinosum* in Northwestern Patagonia grasslands. Plant Ecol. 221 (5). https://doi.org/10.1007/s11258-020-01020-5.

Troncoso, C., Green, D., Reinoso, F., 2020. Experiencia en la propagación de llareta (*Azorella compacta* Phil., Apiaceae), en Collahuasi, comuna de Pica, Región de Tarapacá. Chile Chloris Chil. 23 (1), 148–159. ⟨www.chlorischile.cl⟩.